Novell Closed-Form Equations for Optimum Pressure Ratio and Critical Pressure by Means of Mathematical Modell for Turbojet Engine

FOROOZAN ZARE
Department of Aeronautics, Naval Architecture and Railway Vehicles, Faculty of Transportation Engineering and Vehicle Engineering, Budapest University of Technology and Economic, Hungary, H-1111 Budapest, Műegyetem rkp. 3., e-mail address: fzare@vrht.bme.hu

ÁRPÁD VERESS*
Department of Aeronautics, Naval Architecture and Railway Vehicles, Faculty of Transportation Engineering and Vehicle Engineering, Budapest University of Technology and Economic, Hungary, H-1111 Budapest, Műegyetem rkp. 3., e-mail address: averess@vrht.bme.hu

Abstract
Todays, The turbojet engines are the most relevant propulsion systems for aeronautical applications at low-speed supersonic flow regime between the low by-pass and ramjet engines and they can be considered as a basic of gas turbine engines in respect to introducing advanced mathematical models. Design, development and analysis of such engines can be improved and accelerated by deriving new, simple and closed-form expressions with high accuracy for determining the optimum operational conditions. Hence, the main goal of the present paper is to introduce explicit equations for calculating the optimum pressure ratio, which provides the maximal thrust at real flow conditions. Thermodynamic model for single spool turbojet engines were developed and verified with applying the РД-9Б and АЛ-21Ф3 engines as first steps of the present work. Previously unknown real flow related and technical parameters were identified by constrained optimization. The temperature and component mass fraction dependent gas properties were computed by iteration cycles. A new closed-form expression was derived for determining the critical pressure in choked flow condition at converging nozzle considering losses and process-dependent gas properties. New explicit equations were derived and verified for calculating the optimum total pressure ratio of the compressor pertaining at maximum thrust at chocked and unchocked flow conditions. The presented procedure can also be applied and extended for other type of jet engines and for optimum compressor pressure ratio at thrust specific fuel consumption by means of modifying the used expressions following consistently adapted theoretical derivations.

Keywords
Single spool turbojet engine, thermodynamics, real flow condition, critical pressure, optimum pressure ratio, verification

Nomenclature

Variables (Latin)

A_9 = Outlet area of the exhaust nozzle of engine, m^2

C_p = Specific heat at constant pressure, J/kg/K

---

* Corresponding author

$\bar{C}_p$ = Mean (between T_i and T_{i+1}) specific heat at constant pressure, J/kg/K

f = Fuel to air mass flow rates ratio, -

h = Specific Enthalpy, J/kg

L_0 = Theoretical air mass required to burn 1 kg fuel at stoichiometry condition, kg/kg

$\dot{m}$ = Mass flow rate, kg/s

$\dot{m}_{air}$ = Air mass flow rate entering the engine, kg/s

$\dot{m}_{tech}$ = Bleed air mass flow rate due to technological reasons, kg/s

M = Mach number, -

p = Pressure, Pa

r = Total pressure recovery factor, -

R = Specific gas constant, J/kg/K

T = Temperature, K, Thrust, N

TSFC = Thrust Specific Fuel Consumption, kg/ (kN·h)

V = Flight speed, m/s

W_c = Power requirement of the compressor, W

W_T = Power of the turbine, W

Variables (Greek)

γ = Ratio of specific heats,-

$\overline{\gamma}$ = Ratio of mean specific heats, -

δ_{bc} = Air income ratio due to turbine blade cooling, -

δ_{tech} = Bleed air ratio for technological reasons, -

ξ = Power reduction rate of the auxiliary systems, -

η = Efficiency, -

π = Total pressure ratio, -

Subscripts

0 = Total

0-9 = Engine cross sections

a = Ambient, Afterburner

Al = Afterburner liner

C = Compressor

c = Critical

cc = Combustion chamber

b = Burning

bc = Blade cooling

d = Diffuser

f = Fuel

m = Mechanical

mix = Mass averaged parameter of gas mixture

n = Nozzle

opt = Optimum

s = Isentropic

T = Turbine

1. Introduction

There are many ongoing researches in the field of aeronautics [1], [2]. The application of heat engines is widespread not only in the energy but in the aerospace industry too. A great deal of research has been carried out in analyzing and developing gas turbine system [3], [4], [5] and system components [6], [7].

The gas turbines are currently the only available propulsion systems for high-powered commercial and military airplanes. These engines are also utilized also in other sectors such as oil, gas and energy production. In spite of the fact that their thermodynamic cycles do not have high core thermal efficiency (~ 28 to 38 %) in comparison with piston engines, the jet engines have substantial advantages in overall power, power density (power of the engine compared to the mass of the engine), compactness, streamlining, simplicity and low maintenance cost demands. The jet engines are also less sensitive to overloads and produce less vibration due to the well balanceable and rather axisymmetric rotational components. The gas turbines have high availability (80-99 %), reliability, which can exceed 99 % and low emissions (there is no lubricant in the combustion chamber and no soot during transient loads). It has fewer moving parts and lower sensitivities to fuel composition compared to piston engines [8]. Additionally, jet engines do not need a liquid-based cooling system, although the maximum allowable temperature (~ 1500 C°) at the turbine inlet section is limited for metallurgical reasons [8].

Beside the technical level of gas turbines today, there are many possible areas for potential improvements of their efficiency, power and emissions. Although the experiences and the know-how of the gas turbine manufacturers are increasing continuously, developing more accurate mathematical models for determining the most suitable thermo-dynamical parameters can significantly contribute to decrease cost, time and capacity in the early phases of design and developments. Many scientific publications deal with thermodynamic-based simulation approaches.

Homaifar et al [5] presented an application of genetic algorithms to the system optimization of turbofan engines. The goal is to optimize the thrust per unit mass flow rate and overall efficiency in the function of Mach number, compressor pressure ratio, fan pressure ratio and bypass ratio. Genetic algorithms are used in this article because they are able to quickly optimize the objective functions involving sub functions of multivariate. Although the model used here to represent a turbofan engine is a relatively simple one, the procedure would be exactly the same with a more elaborate model. Results of assorted runs fixed with experimental and single parameter optimization results. Chocked condition was not considered and the air and gas properties were constant or averaged at the given sections of the engine based on the used reference.

Guha [9] determined the optimum fan pressure ratio for separate-stream as well as mixed-stream bypass engines by both numerical and analytical ways. The optimum fan pressure ratio was shown to be predominantly a function of the specific thrust and a weak function of the bypass ratio. The gas properties were considered to be constant in the expression of optimum fan pressure ratio for separate-stream bypass engines at real flow condition.

Silva and his co-workers [10] presented an evolutionary approach called the StudGA which is an optimization design method. The purpose of their work was to optimize the performance of the gas turbine in terms of minimizing fuel consumption at nominal thrust output, and simultaneously to maximize the thrust at the same fuel consumption, as well as to decrease turbine blade temperature. Nozzle efficiency had a direct effect upon thrust. The type and geometry of the inlet and inlet duct was determined the pressure loss and distortion of the air supplied to the engine, which was affected the installed thrust and fuel consumption. Performance optimization of this engine used the effects of these variable geometry devices to establish compromise control configurations, to improve the working conditions.

Mattingly [11] published a detailed theoretical review about the rocket and gas turbine propulsion. There is a description also in that literature how the thermo-dynamical cycles determines the mean characteristic of the jet engines. The author presented a closed-form equation for the optimum compressor pressure ratio at maximum specific thrust at ideal (frictionless) flow condition. The effects of temperature and fuel to air ratio were not considered in parameters describe the gas properties.

The revised sources use simplifications as excluding the effect of chocked flow condition and gas properties with considering the local temperature and fuel to air ratio for example. They also confirm the need for developing more accurate mathematical models, calculations and optimizations.

Single spool turbojet engines are frequently used in commercial and military applications due to their low normalized range factor[1] and low emissions at relatively high flight speed. Two turbojets of this type, the РД-9Б and the АЛ-21Ф3 were thus used for testing and verifying the results of the presently developed mathematical model. The

---

[1] The range factor is the fuel and engine masses are divided by the thrust, which is reduced by the drag force of the nacelle - at given speed and at the given range.

РД-9Б is the first engine, which includes a supersonic stage compressor. This engine is a single-spool axial flow turbojet engine with a nine-stage compressor and an afterburner. It has a bleed air dump control system depending on the compression ratio. Following the compressor, the air flows through can annular combustion chambers mounted in a single cover. The axial flow turbine has two stages, with a hydraulically-regulated nozzle situated behind the afterburner chamber. The РД-9Б was designed as a light, powerful engine for fighter aircraft, and it was used in the MiG-19S, MiG-19P, MiG-19PM and Yak-25 aircraft. The АЛ-21Ф3 turbojet aircraft engine was used in the Sukhoi Su-17, Sukhoi Su-24 and Sukhoi T-10. It can equal the GE J-79 engine as one of the most powerful supersonic engines in service today.

2. Mathematical Model of the Gas Turbine

The description of the applied modeling approach and the results of the thermo-dynamical analyses of the gas turbines are discussed in the present chapter.

2.1. Introduction

A meridian cross section of a typical single spool turbojet engine with afterburner is shown in Figure.1. In the first section “0” represents the ambient conditions.

The ambient parameters of pressure and temperature at static sea level conditions are obtained from the ISA (International Standard Atmosphere):

- Ambient static pressure: $p = p_0$ =101325 Pa
- Ambient static temperature: $T = T_0$ =288 K
- Mach number: $M = 0$

The reason of this start condition (maximum thrust at sea level) is that the engine data were available at that operational mode in the technical specification of the engine [12]. The extension of the below described method can be completed for high flight Mach number in the next step of the present work.

The ambient air from stage “0” enters the engine at cross section “1” and passes through the inlet diffuser until cross section “2”. The pressure recovery rate in the diffuser was considered. The air is then compressed from sections “2 to 3”. The pressure ratio and isentropic efficiency at the compressor was used to determine the total pressure and temperature at the outlet port of the unit. Here, bleed air was considered due to technological reasons. The pressure recovery rate and burning efficiency were applied for real flow modelling in the combustion chamber (which is located between stage “3 and 4”). The mass flow rate of the fuel was determined by the total enthalpy balance of the combustion chamber, taking into account the stagnation enthalpy of the incoming pure air and the fuel, the heat generation of the combustion, the stagnation enthalpy of the hot gas leaving the combustion chamber in a stoichiometric condition, and the stagnation enthalpy of the pure air at the outlet section of the combustion chamber. In order to consider the variation of the gas properties at specific heat at constant pressure, an iteration process was applied to correct the mass flow rate of the fuel by recalculating the specific heat. The incoming mass flow rate of the blade cooling air as it enters into the turbine at the section “4” was also taken into account. The hot gas expands and supplies energy for the turbine, which provides power to the compressor. The power equilibrium of the compressor and turbine spool was used to calculate the total temperature at the outlet section of the turbine. The gas stream leaves the turbine at stage “5” and enters the afterburner to increase the energy of the flow stream by means of adding fuel to a certain amount of the unburnt oxygen. The afterburner is located between cross sections “6 and 7”. Total enthalpy balance was applied to this segment in order to determine the fuel mass flow rate going into the afterburner. Then the expanded gases enter the converging-diverging exhaust nozzle across section “7” and produce thrust leaving the engine at stage “9”. The temperature in the after burner (T_{07}) together with other unknown parameters such as pressure recovery rates and efficiencies – described in the next paragraph – were obtained by a parameter identification.

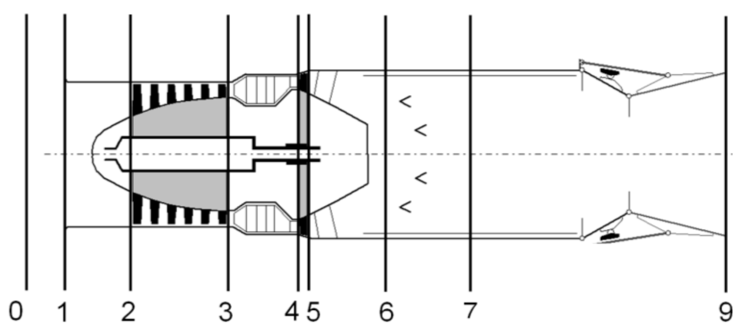

Figure 1. Layout of single spool turbojet engine with afterburner [13]

The input parameters of the mathematical model can be divided into initially known and unknown parameters. The known input parameters are the incoming air mass flow rate, the pressure ratio of the compressor, the total temperature of the turbine inlet and the outlet cross section of the engine. The unknown parameters are the efficiencies (mechanical, isentropic of compressor and turbine, burning and exhaust nozzle), the pressure recovery rates (in the inlet diffuser, combustion chamber and afterburner or turbine exhaust pipe), the power reduction rate of the auxiliary systems, the bleed air ratio for technological reasons, the air income ratio due to blade cooling and the total temperature in the afterburner. Constrained optimization method was applied to determine the unknown parameters by recovering the thrust and thrust specific fuel consumption as the goal function, which parameters were also available in the specification [12].

Beside the unvarying gas properties such as specific gas constants, it is worth taking into consideration the effect of the local temperature and mass fraction consideration when determining the specific heats at constant pressure and the ratios of the specific heats. These variables can be changed not only at each cross section of the engine, but also at different operational conditions in the function of the compressor pressure ratio. Eq. (1) and Eq. (3) show the expressions as they are determined as the mean value by means of each process. Eq. (2) and Eq. (4) presents their standalone values at a given temperatures and fuel to air mass flow ratios. Iteration processes are applied if the temperature and/or mass fractions are the variables of the unknown parameters, so as to gain the equilibrium between the temperature dependent gas properties and the questionable unknown thermodynamic parameters.

$$\bar{C}_{pmix}\left(T_i, T_{i+1}, f\right) = \frac{1000\sum_{j=0}^{n}\frac{a_j + f\,c_j}{(j+1)(f+1)}\left[\left(\frac{T_{i+1}}{1000}\right)^{j+1} - \left(\frac{T_i}{1000}\right)^{j+1}\right]}{T_{i+1} - T_i} \tag{1}$$

$$C_{pmix}\left(T, f\right) = \sum_{j=0}^{n}\frac{a_j + f\,c_j}{f+1}\left(\frac{T}{1000}\right)^{j} \tag{2}$$

$$\bar{\gamma}_{mix} = \frac{\bar{C}_{pmix}\left(T_i, T_{i+1}, f\right)}{\left(T_i, T_{i+1}, f\right) - R_{mix}} \tag{3}$$

$$\gamma_{mix} = \frac{C_{pmix}\left(T, f\right)}{C_{pmix}\left(T, f\right) - R_{mix}} \tag{4}$$

The polynomial constants for air and kerosene fuel are a_j and c_j according to [14]. The values of the polynomial constants of gases are shown in Table1.

The related thermodynamic equations for the each segment of the engine were already published in [15].

2.2. Analysis of Single Spool Turbojet Engines

РД-9Б and АЛ-21Ф3 turbojet engines at start condition (maximum thrust at sea level condition) have been considered for the analyses, for the verification of the simulation method and to test the new equations.

The calculation disciplines which, were described in the previous subchapter, were used for the analysis. The known parameters of the engines are presented in Table 2. However, as noted before, there are also unknown parameters of the engines, which are shown in Table 3 and 4. Hence, an optimization method was used in a Matlab environment in order to determine these unknown parameters via parameter identification. The function used is called “Fmincon”, and the approach is referred to as constrained nonlinear optimization or nonlinear programming, which applies a sequential quadratic programming (SQP) method [16]. In this case, the function solves a quadratic programming (QP) sub problem at each iteration. The method used trials with multiple restarts and repeated these until the maximum function evaluation limit is reached, or until the “Fmincon” algorithm would not significantly improve the current best solutions. The known thrust and thrust specific fuel consumption were the goal functions of the optimization, which were aimed to reach by modifying the unknown parameters over the given ranges. The results and range of each parameter (upper and lower limits) are found in Tables 3-4.

Type of turbojet engine	Known input data, which are used in the simulation			Known available data for parameter identification	
	T_{04} (K)	π_C	$\dot{m}_{air}$ (kg/s)	T (N)	$TSFC$ (kg/(kN h))
Single spool engine (РД-9Б) with afterburner	1150	7.5	43.3	32400	163
Single spool engine (АЛ-21Ф3) with afterburner	1385	15	104	110000	190

Table 2. Available operational data of the РД-9Б and АЛ-21Ф3 turbojet engines at start condition [12]

Type of turbojet engine	Pressure recovery rates and efficiencies of the engine components							
	r_d	r_{cc}	r_{Al}	$\eta_{C,s}$	$\eta_{T,s}$	η_m	η_b	η_n
Single spool turbojet engine with afterburner (РД-9Б)	0.9	0.94	0.91	0.83	0.87	0.995	0.97	0.95
Single spool turbojet engine with afterburner (АЛ-21Ф3)	0.9	0.93	0.89	0.82	0.88	0.99	0.94	0.92
Given ranges for the constrained optimisation	0.88 0.94	0.94 0.97	0.88 0.97	0.81 0.88	0.87 0.94	0.99 0.995	0.94 0.97	0.92 0.96

Table 3. Identified parameters with the ranges of the investigated РД-9Б and АЛ-21Ф3 turbojet engines at start condition

Type of turbojet engine	Power reduction rate of the auxiliary systems, bleed air ratio for technological reasons, air income ratio due to blade cooling and total temperature in the afterburner			
	ξ	δ_{tech}	δ_{bc}	T_{07} (K)
Single spool turbojet engine with afterburner (РД-9Б)	0.005	0.077	0.0534	1700
Single spool turbojet engine with afterburner (АЛ-21Ф3)	0.005	0.07	0.06	1900
Given ranges for the constrained optimisation	0.005 0.01	0.02 0.18	0.05 0.06	1700 2200

Table 4. Identified parameters and ranges of the investigated РД-9Б and АЛ-21Ф3 turbojet engines at start condition

Type of turbojet engines	Available data		Output of the optimization	
	T (N)	$TSFC$ (kg/(kN h))	T (N)	$TSFC$ (kg/(kN h))
Single spool turbojet engine (РД-9Б) with afterburner	32400	163	32420	162.96
Single spool turbojet engine (АЛ-21Ф3)with afterburner	110000	190	110000	190

Table 5. The available and the resulted thrust and thrust specific fuel consumption used in the optimization for parameter identification

Table 5 shows that the output thrust and thrust specific fuel consumption of the optimization are close to the available data. The highest relative differences between the known and the resulted values in the parameter fitting for the thrust is 0.0617 % and for *TSFC* is 0.0245 % at РД-9Б engine, while the unknown parameters are presented in Table 3 and 4 are within the expected intervals.

The thermodynamic cycle including real engine processes of the РД-9Б engine in the T-s diagram is plotted in Figure 2. The curves with smaller thickness represent the constant pressures. The processes between the engine states denoted by numbers are plotted by thicker lines. This visualization effect is the reason for the constant pressure lines going below the process line in case of the pressure decrement just after sections "3" and "6".

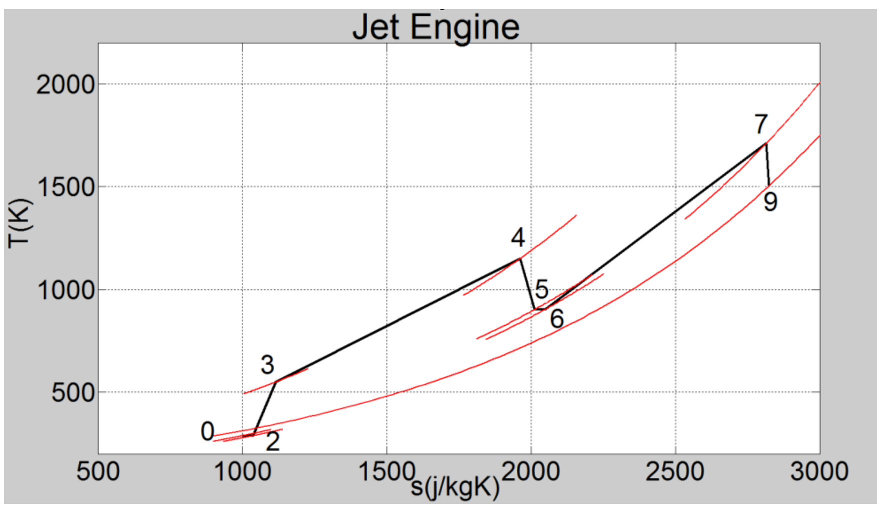

Figure 2. T-s diagram of the РД-9Б turbojet engine with afterburning

3. Optimum Compressor Total Pressure Ratio at Maximum Specific Thrust

New equations have been introduced in the present subchapter for the optimum pressure ratio pertaining at maximum specific thrust. The expressions apply the real (viscous) flow assumptions and the temperature and mass fraction dependencies of the relevant gas properties.

3.1 New Closed-Form Equation to Determine the Optimum Compressor Total Pressure Ratio

The derivation of the optimum pressure ratio at thermodynamic conditions with losses and variable gas properties is based on finding the extreme value of the specific thrust in the function of the compressor pressure ratio. Hence, as the first step, the expression of the thrust is introduced in Eq. (5).

$$T = \left[\dot{m}_9 V_9 - \dot{m}_{air} V_0\right] + A_9\left(p_9 - p_0\right) \tag{5}$$

The mass flow rate at the exhaust nozzle is determined by Eq. (6).

$$\dot{m}_9 = \dot{m}_{air}\left[\left(1-\delta_{tech}\right)\left(1+f_{cc}+f_A\right)\left(1+\delta_{bc}\right)\right] \tag{6}$$

Concerning the well fitted convergent–divergence nozzle, the flow at the exit has ambient pressure, the flow is unchoked and the velocity is supersonic. Because of the considered engines, convergence–divergence nozzle has been considered (see Figure 1.) with correctly expanded flow conditions (p_9=p_0). However, for extending the application range of the equations, the optimum compressor pressure ratio at maximum specific thrust is also derived for only converging nozzle at choked condition.

3.1.1 Unchoked Flow Condition at Converging-Diverging Exhaust Nozzle

As p_9=p_0 only the outlet velocity (V_9) in Eq. (5) depends on the compressor pressure ratio. Hence, the detailed derivation of the expression of the outlet velocity in the function of the compressor pressure ratio is introduced hereafter.

First, the total enthalpy with the mean specific heat at constant pressure is expressed in Eq. (7). This was used to determine the total temperature at the outlet section of the engine.

$$h_{09} = h_9 + \frac{V_9^2}{2} \rightarrow \overline{C}_{pmix}\left(T_{09}, T_9, f\right)T_{09} = \overline{C}_{pmix}\left(T_{09}, T_9, f\right)T_9 + \frac{V_9^2}{2} \rightarrow T_{09} = T_9 + \frac{V_9^2}{2\overline{C}_{pmix}\left(T_{09}, T_9, f\right)} \tag{7}$$

(The fuel to air ratio is calculated based on the overall fuel to air ratio ($f = \left(\dot{m}_{fcc} + \dot{m}_{fa}\right)/(\dot{m}_{air} - \dot{m}_{tech} + \dot{m}_{bc})$)). The fuel to air ratio of the afterburner is also included in f for engines with an afterburner.

The next step is to derive the velocity at the exit of the nozzle by means of thermodynamic condition with losses and variable gas properties in the function of the total pressure ratio of the exhaust nozzle (see Eq. (8)).

$$V_9 = \sqrt{2\overline{C}_{pmix}\left(T_{09}, T_{9s}, f\right)\eta_n T_{09}\left(1 - \frac{1}{\left(\pi_n\right)^{\alpha}}\right)} \tag{8}$$

Parameter α in Eq. (8) is introduced in Eq. (9), and the goal of this simplification is to make the expression of the exhaust velocity more compact. The ratio of specific heats is calculated in the function of the temperature and fuel to air ratio by Eq. (10).

$$\alpha = \frac{\overline{\gamma}_{mix}\left(T_{07}, T_{9s}, f\right) - 1}{\overline{\gamma}_{mix}\left(T_{07}, T_{9s}, f\right)} \tag{9}$$

$$\overline{\gamma}_{mix} = \frac{\overline{C}_{pmix}(T_{09}, T_{9s}, f)}{\overline{C}_{pmix}(T_{09}, T_{9s}, f) - R_{mix}} \tag{10}$$

The total pressure ratio of the nozzle is expressed by the pressure ratio of the compressor and the turbine and the pressure recovery rate of the diffuser, combustion chamber and afterburner liner (see Eq. (11)).

$$r_d \pi_C r_{cc} r_{al} = \pi_T \pi_n \Rightarrow \pi_n = \frac{r_d r_{cc} r_{al} \pi_C}{\pi_T} \tag{11}$$

By substituting Eq. (11) into Eq. (8) the velocity at the exhaust is reformulated as shown in Eq. (12).

$$V_9 = \sqrt{2\overline{C}_{pmix}\left(T_{09}, T_{9s}, f\right)\eta_n T_{09}\left(1 - \left(\frac{\pi_T}{r_d r_{cc} r_{al} \pi_C}\right)^{\alpha}\right)} \tag{12}$$

The power balance of the compressor and turbine spool was used to establish the connection between the total pressure ratio of the compressor and the turbine (see Eq. (13) and (14)).

$$W_C = \eta_m W_T \tag{13}$$

$$\dot{m}_2 \overline{C}_{pmix}\left(T_{02}, T_{03}, f = 0\right)\left(T_{03} - T_{02}\right) = \eta_m \dot{m}_4 \left(1 - \xi\right)\overline{C}_{pmix}\left(T_{04}, T_{05}, f_T\right)\left(T_{04} - T_{05}\right) \tag{14}$$

$\dot{m}_2$ and $\dot{m}_4$ are the mass flow rates in the compressor and turbine respectively and can be expressed in Eq. (15).

$$\dot{m}_2 = \dot{m}_{air},\ \dot{m}_4 = \dot{m}_{air}\left[\left(1 - \delta_{tech}\right)\left(1 + f_{cc}\right)\left(1 + \delta_{bc}\right)\right] \tag{15}$$

Eq. (16) is formed by replacing the mass flow rates in Eq. (14) by Eq. (15), introducing the isentropic efficiencies and isentropic relationship between the temperatures and pressures.

$$\begin{aligned}&\frac{1}{\eta_{C,s}}\overline{C}_{pmix}\left(T_{02},T_{03},f=0\right)T_{02}\left(\left(\pi_C\right)^{\beta}-1\right)=\\&\eta_m\eta_{T,s}\left(1-\delta_{tech}\right)\left(1+\delta_{bc}\right)\left(1+f_{cc}\right)\left(1-\xi\right)\overline{C}_{pmix}\left(T_{04},T_{05},f_T\right)T_{04}\left(1-\frac{1}{\left(\pi_T\right)^{\varepsilon}}\right)\end{aligned} \tag{16}$$

β and ε in the superscripts represent compact forms of the exponents for the isentropic processes in the compressor and the turbine respectively (see Eq. (17)). They are the function of the temperature and the local mass fraction of the air and burnt gases.

$$\beta=\frac{\overline{\gamma}_{mix}\left(T_{02},T_{03s},f=0\right)-1}{\overline{\gamma}_{mix}\left(T_{02},T_{03s},f=0\right)},\qquad \varepsilon=\frac{\overline{\gamma}_{mix}\left(T_{04},T_{05s},f_T\right)-1}{\overline{\gamma}_{mix}\left(T_{04},T_{05s},f_T\right)} \tag{17}$$

Parameter φ is introduced to include all the parameters in Eq. (16) except for ε, π_T, π_c and β and it is shown in Eq. (18).

$$\varphi=\frac{\overline{C}_{pmix}\left(T_{02}T_{03},f=0\right)}{\overline{C}_{pmix}\left(T_{04}T_{03},f_{cc}\right)}\frac{T_{02}}{T_{04}}\frac{1}{\eta_m\eta_{C,s}\eta_{T,s}\left(1-\delta_{tech}\right)\left(1+\delta_{bc}\right)\left(1+f_{cc}\right)\left(1-\xi\right)} \tag{18}$$

Eq. (19) is formed by rearranging Eq. (16) and expressing the total pressure ratio of the turbine.

$$\pi_T=\left(1-\varphi\left(\left(\pi_C\right)^{\beta}-1\right)\right)^{\left(-1/\varepsilon\right)} \tag{19}$$

The velocity at the exhaust of the nozzle (see Eq. (20)) is found by substituting Eq. (19) into Eq. (12).

$$V_9=\sqrt{2\overline{C}_{pmix}\left(T_{09},T_{9s},f\right)\eta_n T_{09}\left[1-\left(\frac{1}{\left(1-\varphi\left(\left(\pi_C\right)^{\beta}-1\right)\right)^{\frac{1}{\varepsilon}}\pi_C\kappa}\right)^{\alpha}\right]} \tag{20}$$

κ in Eq. (20) represents the multiplication of the pressure recovery rate in the diffuser, in the combustion chamber and in the afterburner liner ($\kappa=r_d r_{cc} r_{al}$).

Finally, the specific thrust is expressed by inserting Eq. (20) into Eq. (5) at the start condition (see Eq. (21)).

$$\frac{T}{\dot{m}_{air}}=\left[(1-\delta_{tech})(1+f_{cc}+f_a)(1+\delta_{bc})\right]\sqrt{2\bar{C}_{pmix}(T_{09},T_{9s},f)\eta_n T_{09}\left[1-\left(\frac{1}{\left(1-\varphi\left((\pi_C)^{\beta}-1\right)\right)^{\frac{1}{\varepsilon}}\pi_C\kappa}\right)^{\alpha}\right]}$$

(21)

The objective of the optimization process is to determine the optimum pressure ratio of the compressor which pertains to maximum specific thrust. The reason of considering the specific thrust (thrust per unit mass flow rate of air) is to exclude the effect of compressor pressure ratio on the mass flow rate of air. The condition for the maximum specific thrust is shown by Eq. (22).

$$\frac{\partial\left(\frac{T}{\dot{m}_{air}}\right)}{\partial\pi_C}=0 \tag{22}$$

Two sub steps of the derivation process are shown in the next two equations.

$$\frac{\partial\left(\frac{T}{\dot{m}_{air}}\right)}{\partial\pi_C}=-\frac{1}{2}\frac{\begin{gathered}\left[(1-\delta_{tech})(1+f_{cc}+f_a)(1+\delta_{bc})\right]\left[\frac{1}{\left(1-\varphi\left((\pi_C)^{\beta}-1\right)\right)^{\frac{1}{\varepsilon}}\pi_C}\right]^{\alpha}\cdot\\ \cdot\,\alpha\left[\begin{gathered}\frac{\varphi(\pi_C)^{\beta}\beta}{\left(1-\varphi\left(\left((\pi_C)^{\beta}-1\right)\right)\right)^{\frac{1}{\varepsilon}}(\pi_C)^{2}\varepsilon\left(1-\varphi\left(\left((\pi_C)^{\beta}-1\right)\right)\right)}\\ -\frac{1}{\left(1-\varphi\left((\pi_C)^{\beta}-1\right)\right)^{\frac{1}{\varepsilon}}(\pi_C)^{2}}\end{gathered}\right]\left(1-\varphi\left((\pi_C)^{\beta}-1\right)\right)^{\frac{1}{\varepsilon}}(\pi_C)\end{gathered}}{\sqrt{1-\left[\frac{1}{\left(1-\varphi\left((\pi_C)^{\beta}-1\right)\right)^{\frac{1}{\varepsilon}}(\pi_C)}\right]^{\alpha}}} \tag{23}$$

$$\frac{\partial\left(\dfrac{T}{\dot{m}_{air}}\right)}{\partial\pi_C}=\frac{1}{2}\frac{\left[(1-\delta_{tech})(1+f_{cc}+f_a)(1+\delta_{bc})\right]\left[\dfrac{\left(1-\varphi(\pi_C)^{\beta}+\varphi\right)^{\frac{-1}{\varepsilon}}}{(\pi_C)}\right]^{\alpha}\alpha\left(\varphi(\pi_C)^{\beta}\beta-\varepsilon+\varepsilon\varphi(\pi_C)^{\beta}-\varepsilon\varphi\right)}{(\pi_C)\sqrt{1-\left[\dfrac{\left(1-\varphi(\pi_C)^{\beta}+\varphi\right)^{\frac{-1}{\varepsilon}}}{(\pi_C)}\right]^{\alpha}}\;\varepsilon\left(-1+\varphi(\pi_C)^{\beta}-\varphi\right)}$$

(24)

After completing the derivation and performing arrangements and simplifications, the final form of the optimum pressure ratio is presented in Eq. (25).

$$\pi_{C\_opt}=\sqrt[\beta]{\frac{\varepsilon(1+\varphi)}{\varphi(\varepsilon+\beta)}} \tag{25}$$

3.1.2 Choked Flow Condition at Converging Exhaust Nozzle

Although converging-diverging nozzle is used for such engines (РД-9Б and АЛ-21Ф3) as it is shown in Fig. 1. the extension of the method is discussed in the present section for increasing the application range of the method for converging type nozzle at choked flow condition.

A similar process was applied to evaluate the optimum pressure ratio of the compressor in a choked condition as it was before. The velocity at the exit of the converging nozzle is the speed of sound, when it is in a choked condition at converging nozzle and it is not a function of the compressor pressure ratio explicitly. However, beside the exhaust velocity, the exhaust pressure also contributes to generating thrust (see p_9 in Equation (5)). This pressure is the critical pressure and can also be expressed in the function of the compressor pressure ratio as it is going to be shown below. The total pressures at the inlet and at the outlet section of the turbine are calculated by Eq.s (26) and (27) respectively.

$$p_{04}=r_{cc}\pi_C p_{02} \tag{26}$$

$$p_{05}=\frac{p_{04}}{\pi_T}=\frac{r_{cc}\pi_C p_{02}}{\left(1-\varphi\left((\pi_C)^{\beta}-1\right)\right)^{-\frac{1}{\varepsilon}}} \tag{27}$$

The total pressure at the inlet section of the nozzle (see Eq. (28)) is determined by the turbine outlet total pressure and the total pressure recovery rate of the afterburner liner.

$$p_{07} = r_{al} p_{05} = \frac{r_{cc} r_{al} \pi_C p_{02}}{\left(1-\varphi\left(\left(\pi_C\right)^{\beta}-1\right)\right)^{-\frac{1}{\varepsilon}}} \tag{28}$$

The total enthalpy and subsequently the total temperature at section 9 is introduced in the next steps (see Eq. (29-30)).

$$h_{09} = h_9 + \frac{V_9^2}{2} \rightarrow \overline{C}_{pmix}\left(T_{09}, T_9, f\right) T_{09} = \overline{C}_{pmix}\left(T_{09}, T_9, f\right) T_9 + \frac{V_9^2}{2} \rightarrow T_{09} = T_9 + \frac{V_9^2}{2\overline{C}_{pmix}\left(T_{09}, T_9, f\right)} \tag{29}$$

$$T_{09} = T_9 + \frac{1}{\overline{C}_{pmix}\left(T_{09}, T_9, f\right)} \frac{V_9^2}{2} \frac{a_9^2}{a_9^2} \Rightarrow T_{09} = T_9 + \frac{1}{\overline{C}_{pmix}\left(T_{09}, T_9, f\right)} M_9^2 \frac{\gamma_{mix}\left(T_9, f\right) R T_9}{2} \tag{30}$$

The critical condition corresponds to M_9=1 and $T_9 = T_c$, so the Eq. (30) is reformulated according to this. The isentropic static temperature at point 9 is expressed by the equation of isentropic nozzle efficiency and it is given by Eq. (31).

$$T_{9s} = T_{09} - \frac{1}{\eta_n} \frac{\left(T_{09} - T_C\right) \overline{C}_{pmix}\left(T_{09}, T_C, f\right)}{\overline{C}_{pmix}\left(T_{09}, T_{9s}, f\right)} \tag{31}$$

The thermodynamic process between point 7 and 9s is isentropic as shown in Eq. (32).

$$\frac{p_C}{p_{07}} = \left(\frac{T_{9s}}{T_{09}}\right)^{\frac{\overline{\gamma}_{mix}\left(T_{09}, T_{9s}, f\right)}{\overline{\gamma}_{mix}\left(T_{09}, T_{9s}, f\right)-1}} \tag{32}$$

A new closed-form expression is introduced to determine the critical pressure at the exit of the nozzle after substituting the isentropic static temperature in Eq. (31) and the total temperature at nozzle exit in Eq. (30) into Eq. (32), in which, beside the dependencies of temperature variations and fuel to air ratios in the specific heats at constant pressure, the ratios of the specific heats are also considered. While the critical static pressure at the outlet section of the exhaust system is coupled with the total and static exit temperatures, iteration cycles are used to determine the corresponding critical pressure and the total and static temperatures which are obtained by satisfy Eq. (33) and provide thermodynamic parameters for the engine in a choked condition. This equation for example gives higher critical pressure by 9.3 % for the РД-9Б engine than its original form with constant material data (the ratio of

$$p_9 = p_C = p_{07}\left[1-\frac{1}{\eta_n}\left(1-\frac{2\overline{C}_{pmix}\left(T_{09,}T_C,f\right)}{2\overline{C}_{pmix}\left(T_{09,}T_C,f\right)+\gamma_{mix}\left(T_C,f\right)R_{mix}}\right)\frac{\overline{C}_{pmix}\left(T_{09,}T_C,f\right)}{2\overline{C}_{pmix}\left(T_{09,}T_C,f\right)}\right]^{\frac{\overline{\gamma}_{mix}\left(T_{09},T_{9s},f\right)}{\overline{\gamma}_{mix}\left(T_{09},T_{9s},f\right)-1}} \tag{33}$$

specific heats for gas =1.33 and for the air=1.4).

By substituting Eq. (28) in Eq. (33) and Eq. (33) in Eq. (5) the thrust can be expressed as follows:

$$\begin{aligned} T &= \left[\dot{m}_9 V_9 - \dot{m}_{air} V_0\right] + \\ A_9 &\left[\left(\begin{aligned} & p_{02}\left(r_{cc} r_{al} \pi_C\right)\left(1-\varphi\left(\left(\pi_C\right)^{\beta}-1\right)\right)^{\frac{1}{\varepsilon}} \cdot \\ & \cdot\left[1-\frac{1}{\eta_n}\left(1-\frac{2\overline{C}_{pmix}\left(T_{09,}T_C,f\right)}{2\overline{C}_{pmix}\left(T_{09,}T_C,f\right)+\gamma_{mix}\left(T_C,f\right)R_{mix}}\right)\frac{\overline{C}_{pmix}\left(T_{09,}T_C,f\right)}{2\overline{C}_{pmix}\left(T_{09,}T_C,f\right)}\right]^{\frac{\overline{\gamma}_{mix}\left(T_{09},T_{9s},f\right)}{\overline{\gamma}_{mix}\left(T_{09},T_{9s},f\right)-1}} \end{aligned}\right) - p_0\right] \end{aligned} \tag{34}$$

The determination of the optimum pressure ratio pertaining at maximum thrust in choked converging nozzle flow conditions begins by completing the derivation presented in Eq. (22).

$$\frac{\partial T}{\partial \pi_C} = \left(\left(1-\varphi\left(\pi_C\right)^{\beta}+\varphi\right)^{\frac{1}{\varepsilon}} - \frac{\left(1-\varphi\left(\pi_C\right)^{\beta}+\varphi\right)^{\frac{1}{\varepsilon}}\varphi\left(\pi_C\right)^{\beta}\beta}{\varepsilon\left(1-\varphi\left(\pi_C\right)^{\beta}+\varphi\right)}\right) \tag{35}$$

$$\frac{\partial T}{\partial \pi_C} = \left(\frac{\left(1-\varphi\left(\pi_C\right)^{\beta}+\varphi\right)^{\frac{1}{\varepsilon}}\varepsilon - \left(1-\varphi\left(\pi_C\right)^{\beta}+\varphi\right)^{-\frac{-1+\varepsilon}{\varepsilon}}\varphi\left(\pi_C\right)^{\beta}\beta}{\varepsilon}\right) \tag{36}$$

Completing the arrangements and simplifications, the final form of the expression for the optimum compressor total pressure ratio is given by Eq. (37).

$$\pi_{C\_opt} = \sqrt[\beta]{\frac{\varepsilon\left(1+\varphi\right)}{\varphi\left(\varepsilon+\beta\right)}} \tag{37}$$

Based on Eq. (25) and (37) the optimum pressure ratios for the convergent-divergent nozzle at correctly expanded flow conditions (p_9=p_0 and no shock waves form) and only convergent nozzle at choked conditions are the same. This new closed-form explicit expression involves simplifications, because the gas properties and unknown variables – including efficiencies, pressure recovery rates and specific heats – and the incoming mass flow rate of air in case of choked converging nozzle are considered to be constant in the derivation process. Due to the lack of information, the presented approximation uses the same recovery rates, efficiencies, power reduction rate of the auxiliary systems, bleed air ratio and air income ratio due to the blade cooling for the all pressure ratios. The temperature and component mass fraction dependent gas properties are also considered to be constants during the derivation process.

3.1 Numerical Representation – Verification of the New Equation

The goal of the present subchapter is to verify the correctness and the accuracy of the new expression for the optimum compressor total pressure ratio. Hence, a numerical representation of the optimum pressure ratio was completed. In this context, the numerical representation is a searching algorithm over the expected pressure ratio range, in order to determine the total pressure ratio pertaining at maximum thrust. The same calculation method and the same parameters are used in the new expressions and in the numerical representation, which includes the application of the real (viscous) flow properties. The loss coefficients and other parameters which were previously unknown, and are determined by the constrained optimization based on the available engine data, can change at different operational conditions and at different pressure ratios. However, in this article, these variations are not considered, and all of these unknown parameters are assumed to be constant at all pressure ratios except for the isentropic compressor efficiency which is the function of fixed polytrophic efficiency and compressor total pressure ratio for the fixed technology level

Figure 3. shows the compressor pressure ratio-thrust function as numerical representation.

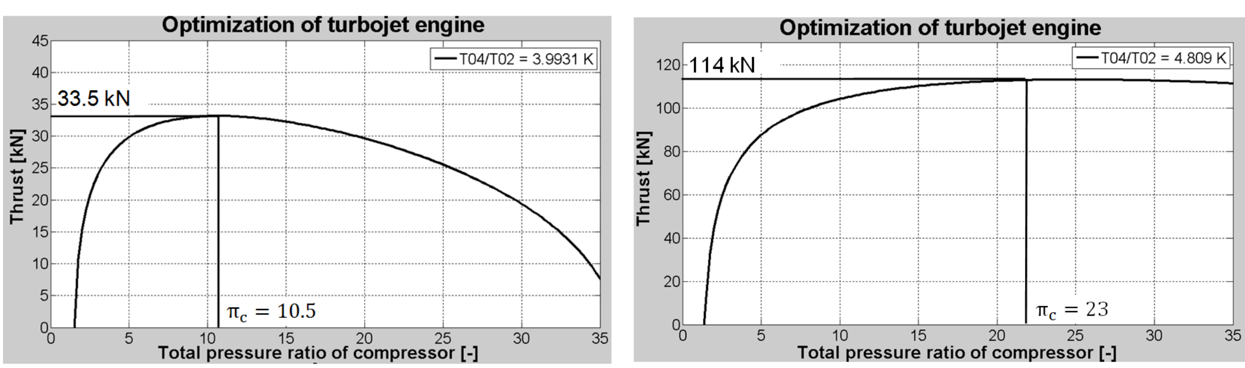

Figure 3. Thrust vs. total pressure ratio of the compressor for РД-9Б (left) and АЛ-21Ф3 (right) turbojet engines with afterburner

The optimum pressure ratios are 10.5 and 23 at maximum thrust 33500 N and 114000 N for РД-9Б and АЛ-21Ф3 respectively in the numerical representations. The optimum pressure ratio of the compressors, provided by Eq. (25 and 37), are 10.2 and 22.8, and the maximum thrusts are 33680 N and 114400 N for the РД-9Б and АЛ-21Ф3 jet engines. The highest difference between the maximum thrusts using a numerical method and using the new equation is 0.54 %. This deviation is due to the fact that the specific heats at constant pressure and parameters correspond to certain operational modes and the real flow assumptions in the specific thrust and thrust equations (Eq. (21 and 34)) are assumed to be constant during the derivation. However, the resulting difference is negligible and the results are accepted in engineering point of view.

The specific thrusts in the function of compressor total pressure ratios for the both engines are shown in case of correctly expanded converging-diverging nozzle flow conditions and at different T04/T02 ratios in Figure 4. Higher turbine inlet temperature increases the specific thrust and the maximum values of that belong to higher compressor total pressure ratios.

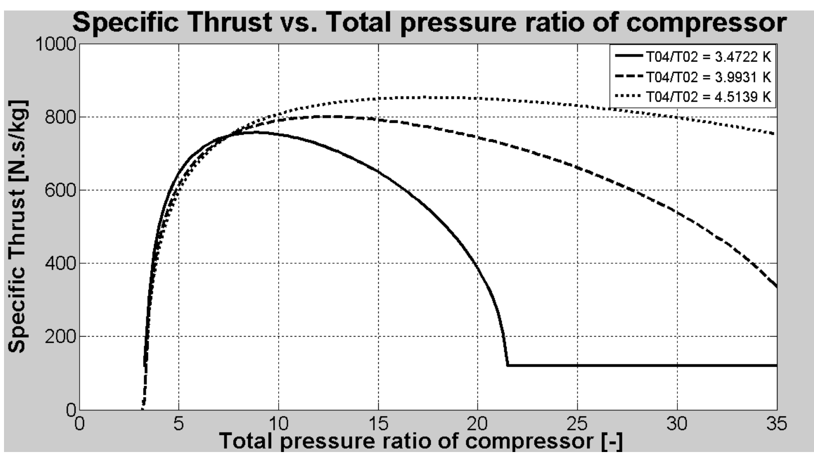

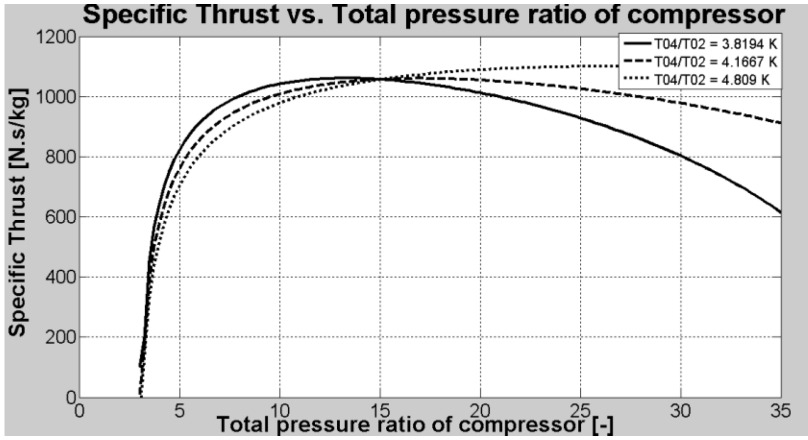

Figure 4. Specific thrust vs. total pressure ratio of the compressor for РД-9Б (above) and АЛ-21Ф3 (below) turbojet engines with afterburner

The thrust specific fuel consumption in the function of compressor total pressure ratio for the both engines are shown in case of correctly expanded converging-diverging nozzle flow conditions and at different T04/T02 ratios in Figure 5. The maximum specific thrust and minimum *TSFC* belong to the same compressor total pressure ratio ranges for the both investigated cases, which is in correlation with reference [11].

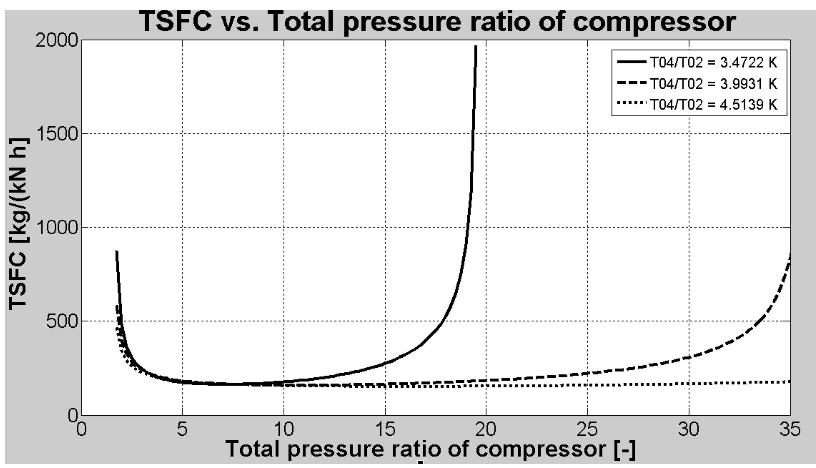

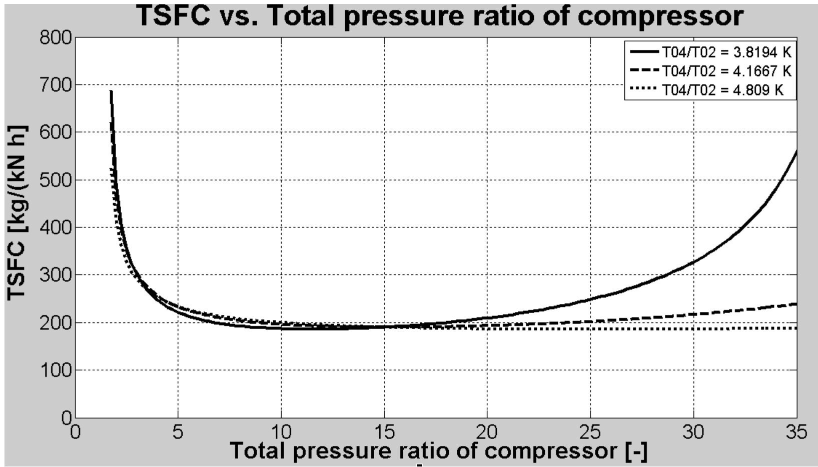

Figure 5. *TSFC* vs. Total pressure ratio of compressor for РД-9Б (up) and АЛ-21Ф3 (down) turbojet engines with afterburner

In order to determine the effect of considering the pressure recovery factors, efficiencies and parameter dependent specific heat for the thermodynamic cycle, for the optimum pressure ratio and so for the thrust of a single spool turbojet engine, four different test scenarios were performed. The results of this investigation are found in Table 6. The ☑ sign in the column of viscous flow conditions means that the pressure recovery factors and efficiencies are considered in the calculation, meanwhile ☒ represent that it does not.

	Real flow conditions	Gas properties	π_c РД-9Б first and АЛ-21Ф3 second		Max. Thrust (РД-9Б first and АЛ-21Ф3 second) [kN]	
Present optimization study Eq.s (25 and 37)	☒	Dependent function by the fuel to air ratio of gas mixture and temperature	29	52	69.3	242.1
	☒	Constant	27	47	66.4	220
	☑	Dependent function by the fuel to air ratio of gas mixture and temperature	10.5	23	33.5	114
	☑	Constant	9.5	20	32.9	111.3

Table 6. The effect of gas properties (with and without temperature and fuel to air ration dependencies) and real flow conditions (pressure recovery factors and efficiencies) for the optimal pressure ratio and thrust for the РД-9Б and АЛ-21Ф3 single spool turbojet engines

In case of the real flow conditions and variable specific heats, which are included in the Eq.s (25, 37), the optimum pressure ratio is relatively close to the given data in [12]. 40 % and 53.34 % increment can be observed in case of using the new equation, which corresponds to 3.39 % and 3.63% thrust rising for РД-9Б and АЛ-21Ф3 jet engines respectively. In addition, besides keeping the viscous flow assumption, if the specific heat is defined to be constant, there was 9.52 % and 13.04% decrement in the total pressure ratio for РД-9Б and АЛ-21Ф3 jet engines respectively. The non-real flow conditions – as non-viscous and irrotational assumptions – provide unrealistic results; the thrust becomes double in comparing that with the plausible approach. The best and the most realistic test scenario for having the maximum thrust is given by case that pressure recovery rates and efficiencies are considered and the specific heats are assumed to be dependent functions of temperatures and fuel to air ratios.

The condition presented in equation (22) is not sufficient to guarantee that the identified point is of the maximum thrust. The second derivative should also be checked. However, by having the same result of analytical and numerical methods, it represents that it is not necessary to investigate the second derivative.

4. Conclusions

New closed-form expressions were derived in the present research to determine the critical pressure and the optimum compressor total pressure ratios, which provides the maximum thrust of single spool turbojet engines in realistic thermodynamic (frictional flow) conditions.

The concentrated parameter distribution type method was used to model the thermodynamic processes of the two test engines under consideration as РД-9Б and АЛ-21Ф3. The unknown parameters as efficiencies, pressure recovery rates, bleed air ratio, blade cooling mass flow rate and power reduction rate of the auxiliary system, were determined by constrained optimization in terms of minimizing the differences between the calculated and the available thrust and *TSFC* at correctly expanded flow condition in convergent–divergence nozzle. A new equation was derived to determine the optimum compressor pressure ratio pertaining at maximum specific thrust. In order to increase the application range of the new equation, a new closed-form expression was developed also for determining the critical pressure in case of choked nozzle flow condition at converging nozzle. The optimum total pressure ratio was derived also for this operational mode.

The plausibility of the new equation for the optimum total pressure ratio was verified by determining the extreme value of the pressure ratio-thrust functions numerically. The new equation for the optimum pressure ratio provides 3.39 % and 3.63% thrust increment for the РД-9Б and АЛ-21Ф3 jet engines.

Parameter sensitivity analyses were also completed to determine the effect of variable specific heat and viscous flow conditions (pressure recovery rates and efficiencies). The most plausible results appeared in case of viscous flow conditions and variable specific heats at constant pressure by temperature and fuel to air ratio. Here, 9.52 % and 13.04% improvements were observed in the optimum total pressure ratio for the РД-9Б and АЛ-21Ф3 jet engines.

The presented modeling process and the new equations provide not only more accurate results for physical and technical processes and but decrease the time for design, development and analysis of turbojet jet engines beside providing common platform for extending them for other type of engines too.

Acknowledgements

This work was supported by Hungarian national EFOP-3.6.1-16-2016-00014 project titled by " Investigation and development of the disruptive technologies for e-mobility and their integration into the engineering education”.

Bibliography

[1] M. Voskuilj, D. Rohács, J. Rohács, R. J. Schousttra, "Preliminary evaluation of the environmental impact related to aircraft take-off and landings supported with ground based (MAGLEV) power," in *Proceedings of the 4th Annual International Air Transport and Operations Symposium (ATOS)*, Toulouse, French, 2014.

[2] J. Bera, L. Pokorádi, "Monte-Carlo Simulation of Helicopter Noise," *Acta Polytechnica Hungarica,* vol. 12, no. 2, pp. 21-32, 2015.

[3] R. Andoga, L. Főző, L. Madarász, T. Karol, " A digital diagnostic system for a small turbojet engine," *Acta Polytechnica Hungarica,* vol. 10, no. 4, pp. 45-58, 2013.

[4] H. N. Somehsaraei, M. M. Majoumerd, P. Breuhaus, M. Assadi, "Performance analysis of a biogas-fueled micro gas turbine using a validated thermodynamic model," *Applied Thermal Engineering,* vol. 66, no. 1-2, pp. 181-190, 2014.

[5] A. Homaifar, Y. H. Lai, E. McCormick, "System optimization of turbofan engines using genetic algorithms," *Appl. Math. Modelling,* vol. 18, 1994.

[6] K. Beneda, J. Rohács, "Dynamic model of variable inducer shroud bleed for centrifugal Compressor Surge Suppression," *Review of Aerospace Engineering,* vol. 6, no. 3, pp. 163-173, 2013.

[7] K. Beneda, "Development of a modular FADEC for small scale turbojet engine," in *IEEE 14th International Symposium on Applied Machine Intelligence and Informatics*, Herl'any, 2016.

[8] K. Beneda, Gy. Simongáti, Á. Veress, Járművek hő- és áramlástechnikai berendezései I, 1 ed., Budapest: Typotex Kiadó, 2012, pp. Chapter 3, 77.

[9] A. Guha, "Optimum fan pressure ratio for bypass engines with separate or mixed exhaust streams," *Journal of propulsion and power*, vol. 17, no. 5, pp. 1117-1122, 2001.

[10] V. V. R. Silva, W. Khatib, P. J. Fleming, "Performance optimization of gas turbine engine," *Artificial Intelligence*, vol. 18, no. 5, pp. 575-583, 2005.

[11] J. D. Mattingly, K. M. Boyer, "Elements of Propulsion: Gas Turbines and Rockets," *AIAA Education Series*, 2006.

[12] В. В. КУЛАГИН and others, Теория расчёт и проектирование авиационных двигателей и энергетических установок. Книга 1, 2, Moscow, 2005, p. 438.

[13] J. Kurzke, "The GasTurb Program - Commercial computer program, GasTurb12," 2016. [Online]. Available: http://www.gasturb.de.

[14] I. Sánta, "Gázturbinás Repülőgép Hajtóművek," BME Repülőgépek és Hajók Tanszék, Tanszéki jegyzet (Notes on Jet Engines at BME University), Budapest, 2008.

[15] F. Zare, Á. Veress, "Development and Verification of an Improved Thermo Dynamical Model for Single Spool Jet Engines," *Repüléstudományi Közlemények (Publications in Aeronautical Sciences) on-line scientific journal*, vol. XXVI, no. 2, pp. 539-551, 2014.

[16] Mathworks, "Matlab R2017b Documentation (Optimization Toolbox; "fmincon" function)," 2017. [Online]. Available: https://uk.mathworks.com/help/optim/ug/fmincon.html. [Accessed 30 09 2017].